Development Towards Non-invasive Breast Cancer Imaging Using Novel Estrogen Conjugates Fluorescent Dye

Francis K J[1], Iven Jose[2]
Christ University[1,2]
Christ University, Bangalore, Karnataka, India 560029
francis.kj@ece.christuniversity.in

Abstract: Determination of Estrogen Receptor [ER] status is a key in detecting cancer pathogenesis at early stage. In our work we discuss Near Infrared Fluorescence [NIRf] Molecule Optical Imaging Diagnostic modality for early detection of breast cancer. A novel target-specific NIRf dye conjugate aimed at measuring Estrogen Receptor[ER] status was synthesized by ester formation between 17-β estradiol and a hydrophilic derivative of Indocyanine Green (ICG) cyanine dye, bis-1,1-(4-sulfobutyl) indotricarbocyanine-5-carboxylic acid, sodium salt. In-vitro studies regarding specific binding and endocytocis of the dye performed on ER+ve [MCF-7] and control [MDA-MB-231] adenocarcinoma breast cancer cell lines clearly indicated nuclear localization of the dye for MCF-7 as compared to plasma level staining for MDA-MB-231.Furthermore, MCF-7 cells showed ~4.5-fold increase in fluorescence signal intensity compared to MDA-MB-231.

A phantom model is created in COMSOL to study the *in-vivo* efficiency of the dye. It is exited with point source modeling laser diode and fluency at the boundary is calculated with Standard Diffusion Approximation. A model with inclusions imitating property of cancerous cell is used for measurement set alone and another model of homogenous optical property is taken as the initial set for inverse solving. Both the excitation (754nm) and emission (787nm) equations are inverted using iterative Levenberg–Marquardt method with Tikhonov minimization of measured and calculated fluence error. The reconstruction is based on independent solving of excitation and emission equation separating the originally dependant equations. The result of reconstructed absorption and scattering properties were recorded. The computing time was reduced in fully coupling compared to the segregation coupling which are shown in the result. We conclude by stating that this lipophilic dye can be potentially used as a target specific exogenous contrast agent in molecular optical imaging for early detection of breast cancer.

Keywords: Estrogen Receptor, NIR fluorescence, early detection, Inverse problem.

1. Introduction

According to American Cancer Society reports in 2011 shows 230,480 new cases of invasive breast cancer have been diagnosed among women, as well as 57,650 additional cases of in situ breast cancer. Approximately 39,520 women died from breast cancer. So, early detection of breast cancer is the key for effective treatment, which can considerably reduce the death rate. Though other modalities like X-Ray, CT Scans, MRI Scans, PET, and ultrasound is already in use, Diffuse Optical Tomography (DOT) is gaining importance because DOT modality is inexpensive, non-invasive (low energy-non-ionizing), portable and low-power consumption. DOT is also developing as an add-on to existing modalities. NIR optical tomography use therapeutic window of 700nm to 900nm laser beam for interrogating tissue, in which tissue exhibit low absorbance but high scattering capacity. The cancerous tissue detection using NIR light depend critically on the consistent difference between the absorption and scattering properties of normal and diseased tissue volume.

Recently many research groups have been working on fluorescent NIR optical tomography especially using target specific fluorescents. As most of the breast cancers are hormone dependent, hence determination of the hormonal receptor status gains paramount importance when deciding the treatment regime for the patient. Since proliferations of the breast cancer cells are often driven by estrogen, we focus on to developing a technique to detect estrogen receptor status. NIR fluorescent dye conjugate (NIRFDC), which could potentially be used to detect estrogen receptors has been synthesized. The ester developed was tested on the breast cancer cell lines MCF-7/MDA-MB-231 and were found to be non-toxic. In-vitro studies

regarding specific binding and endocytocis of the dye performed on ER+ve [MCF-7] and control [MDA-MB-231] adenocarcinoma breast cancer cell lines clearly indicated nuclear localization of the dye for MCF-7 as compared to plasma level staining for MDA-MB-231.Furthermore, MCF-7 cells showed ~4.5-fold increase in fluorescence signal intensity compared to MDA-MB-231 [4].

A typical DOT system often consists of a laser source, illuminating the biological tissue from the surface at different source positions in succession. The photons which propagate through the tissue are then collected at multiple detector positions on the tissue surface. Three measurement schemes are used for these measurements: time domain, frequency domain and continuous wave. Frequency domain measurement is an optimum scheme with respect to computation complexity and hardware [9]. In our work we present frequency domain measurement with simulated phantom with synthetic measurement i.e., measurement is taken by forward solving in a phantom model and artificial random noise is added to mimic measurement error [5].

In this work we present 3D imaging system model developed in COMSOL Multiphysics. Forward problem is solved using Standard diffusion approximation for both excitation and emission equation and is visualized in 2D slices. 2D slices are reconstructed in NIRFAST (Near Infrared Fluorescence and Spectral Tomography) [1 &2] Software to get absorption and reduced scattering properties. Fluorescent reconstruction is carried out by independent inverting of excitation and emission equation and subtraction of optical properties to get dye properties and location which in turn provide information about diseased tissue area.

2. Synthesis, characterization and in-vitro results of novel dye.

NIR fluorescent dye conjugate (NIRFDC), which could potentially be used to detect estrogen receptors was synthesized. The conjugate was synthesized by ester formation between 17-β estradiol and a cyanine dye namely: bis-1, 1-(4-sulfobutyl) indotricarbo cyanine -5-carboxylic acid, sodium salt. The cyanine dye is a hydrophilic derivative of Indocyanine green (ICG). The ester formed was found to have an extra binding ability with the receptor cites as compared to ICG [3]. The complete reaction for synthesis of NIRFDC is shown in figure1.

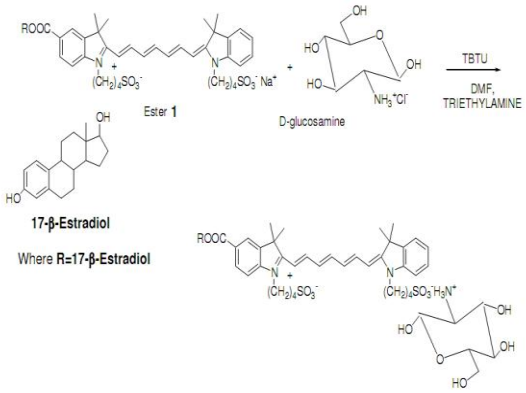

Figure 1. Reaction for synthesis of NIRFDC.

The absorption and fluorescence spectra of synthesized NIRFDC are shown in figure 2 &3. It is evident that the absorption of NIR light by the dye is peaking at 754nm which forms the excitation wavelength and the reemission is at 787nm [4]. The peaks are non-overlapping with the absorption peaks of water, oxy-hemoglobin and deoxy-hemoglobin which eliminate the requirement of reconstruction for those components.

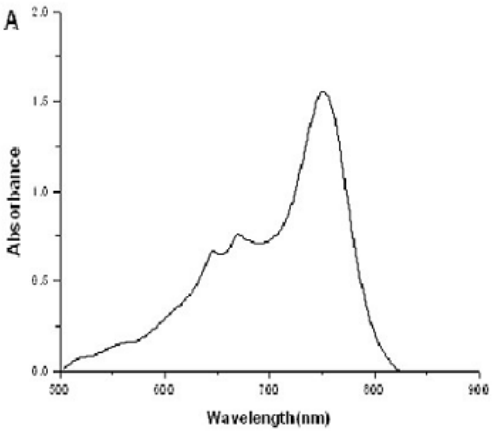

Figure 2. Absorption spectra of NIRFDC.

In-vitro studies were conducted [3] on mammary epithelial cells MCF-7 and MDA-MB-231 breast cancer cell lines as control.

MCF-7 cells shows ~4.5-fold increase in fluorescence signal intensity compared to MDA-MB-231. Florescence quantum yield of the dye is 0.114 and Molar extinction coefficient of dye 6.25e5 M−1 cm−1.

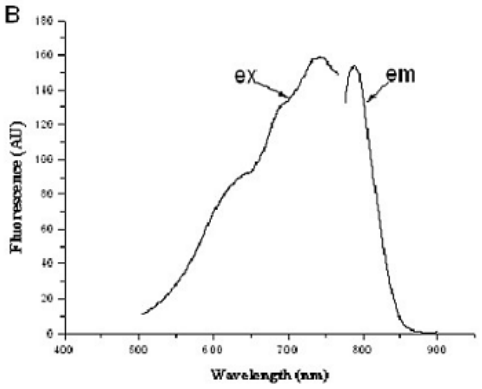

Figure 3. Fluorescence spectra of NIRFDC.

3. Methodology

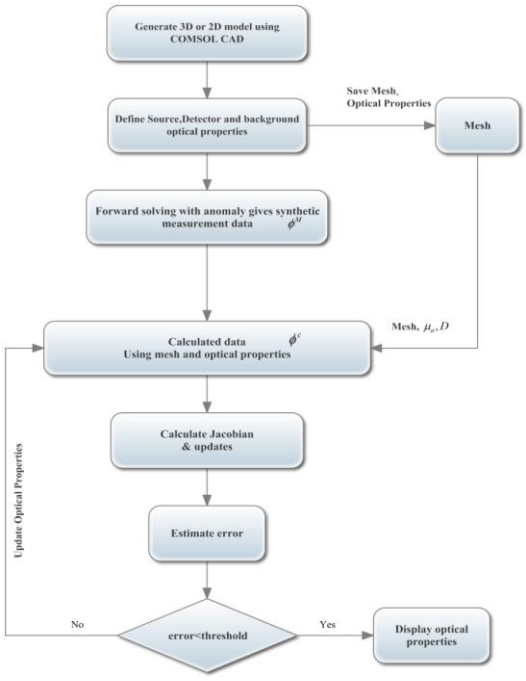

Figure 4. Flowchart showing reconstruction process.

As shown in figure 4, the Phantom model is generated using COMSOL CAD features where the source detector locations and background optical properties are defined. This data is saved as a mesh file. Synthetic data is obtained by forward solving the generated phantom model with anomaly at required location and optical property, this forward solving is done in a finer mesh to increase accuracy of synthetic data.

With the coarser mesh and initial optical properties the forward solving is done in NIRFAST. Jacobian and optical property updates are calculated. The projected error is estimated and compared with the threshold value of error, if error is more, then optical properties are updated and forward solving is continued until error become less than threshold. Finally, the reconstructed optical properties are displayed.

4. Forward Problem

Laser beam interrogation with tissue in NIR window can be modeled using Standard Diffusion Approximation (SDA) or P1 approximation of Radiative Transport Equation (RTE) [5]. The excitation and emission of fluorescent dye can be modeled as two coupled SDA equations. In frequency domain the diffusion equation become elliptical and can be expressed as [6]

$$-\nabla.(D_x\nabla\phi_x(r))+\left[\mu_{axi}+\mu_{axf}+\frac{i\omega}{c}\right]\phi_x(r)=-\Theta_s\delta(r-r_s) \quad (1a)$$

$$-\nabla.(D_m\nabla\phi_m(r))+\left[\mu_{ami}+\frac{i\omega}{c}\right]\phi_m(r)=-\frac{\phi_x(r)\eta\mu_{axf}}{1-i\omega\tau} \quad (1b)$$

$r\in\Omega$

Where

$$D_x=\frac{1}{3(\mu_{axi}+\mu_{axf}+\mu'_{sx})}$$

$$D_m=\frac{1}{3(\mu_{ami}+\mu'_{sm})}$$

The subscript *x* and *m* denote the excitation and emission light wavelengths. Subscript *i* in optical property indicates internal tissue properties and *f* indicates properties introduced due to fluorescent dye injection. μ_a and μ'_s are absorption and reduced scattering coefficient respectively.

$\Theta_s \delta(r - r_s)$ is the excitation light source of power Θ_s and one diffusion length away from boundary. $\phi_{x,m}$ is the photon fluence. η is fluorescent quantum efficiency and τ is fluorescent life time.

Subjected to Robin boundary conditions on the boundary [6]

$$\mathbf{n}.[2A_x D_x \nabla \phi_x(r)] + \phi_x(r) = 0 \quad \forall r \in \partial\Omega \quad (2a)$$

$$\mathbf{n}.[2A_m D_m \nabla \phi_m(r)] + \phi_m(r) = 0 \quad \forall r \in \partial\Omega \quad (2b)$$

Where equation 1a and 1b models excitation light and generation and propagation of fluorescence emitted light respectively, **n** is the normal vector to the boundary $\partial\Omega$, θ_C is the critical angle, A is refractive index mismatch [1] at the boundary given by

$$A = \frac{2/(1-R_0) - 1 + |\cos(\theta_c)|^3}{1 + |\cos(\theta_c)|^2}$$

And

$$R_0 = (n_1 / n_{AIR} - 1)^2 / (n_1 / n_{AIR} + 1)^2$$

Where n_1 is the refractive index of domain and n_{AIR} is the refractive index of air.

5. Independent forward modeling

The coupled equations 1a and 1b can be independently solved using some assumptions [6]. The stoke shift is relatively small and the optical properties of the tissue for two wavelength are similar ie $D_x = D_m = D$ and $\mu_{ax} = \mu_{am} = \mu_a$. Then we can rewrite equation 1a and 1b as

$$-\nabla.(D_x \nabla \phi_x(r)) + \left[\mu_a + \varepsilon_x c(r) + \frac{i\omega}{c}\right]\phi_x(r) = -\Theta_s \delta(r - r_s) \quad (3a)$$

$$-\nabla.(D_m \nabla \phi_m(r)) + \left[\mu_a + \frac{i\omega}{c}\right]\phi_m(r) = -\frac{\phi_x(r)\eta\varepsilon_x c(r)}{1 - i\omega\tau} \quad (3b)$$

Rearranging equation 3(a)

$$\varepsilon_x c(r)\phi_x(r) = \Theta_s \delta(r - r_s) - \left(-\nabla D \nabla + \mu_a(r) + \frac{i\omega}{c}\right)\phi_x(r) \quad (4)$$

Substituting (4) in (3b) we get

$$\left[-\nabla D \nabla + \mu_a(r) + \frac{i\omega}{c}\right]\left(\frac{1 - i\omega\tau}{\eta}\phi_m(r) + \phi_x(r)\right) = \Theta_s \delta(r - r_s) \quad (5)$$

Taking $\frac{1 - i\omega\tau}{\eta}\phi_m(r) + \phi_x(r) = \phi_t(r)$ we can obtain two independent equation

$$\left[-\nabla D \nabla + \mu_a + \varepsilon_x c(r) + \frac{i\omega}{c}\right]\phi_x(r) = -\Theta_s \delta(r - r_s) \quad (6a)$$

$$\left[-\nabla D \nabla + \mu_a(r) + \frac{i\omega}{c}\right]\phi_t(r) = \Theta_s \delta(r - r_s) \quad (6b)$$

This can be separately solved. The entire domain is discretized into piecewise continues polynomial function using basis functions with Finite Element Method (FEM) which is done using COMSOL Multiphysics.

6. Inverse Problem

The goal of inverse problem is to recover optical properties at each node point within the domain using measurements of light fluence at the boundary. If the measurement fluence at tissue surface is represented by ϕ^M and calculated data using forward solver by ϕ^C then standard Tikhonov minimization function [1] is given by

$$\chi^2 = \min_{\mu} \left\{ \sum_{i=1}^{M} (\phi_i^M - \phi_i^C)^2 \right\} \quad (7)$$

Where M is total number of measurements obtained. Minimization with respect to μ is obtained by equating first derivative to zero $\frac{\partial \chi^2}{\partial \mu} = 0$ and ignoring higher order terms

$$\left(\frac{\partial \phi^C}{\partial \mu}\right)^2 (\phi^M - \phi^C) = 0 \qquad (8)$$

$\frac{\partial \phi^C}{\partial \mu}$ is called Jacobian matrix J. Using linear approximation of problem and solving it in an iterative scheme gives [1]

$$(J^T J + \lambda I)\partial\mu = J^T \partial\phi \qquad (9)$$

Where λ is the Tikhonov regularization parameter given by $\lambda = \sigma^2_{\phi^M} / \sigma^2_{\mu}$, $\partial\mu$ is the update of optical properties and $\partial\phi$ is the measurement misfit given by $\phi^M - \phi^C$. Modifying equation (9) to Levenberg-Marquardt (LM) procedure

$$\partial\mu = (J^T J + \bar{\lambda} I)^{-1} J^T \partial\phi \qquad (10)$$

Where $\bar{\lambda} = 2\lambda$. The optical properties are updated using equation (10)

For frequency domain system both amplitude and phase is available so Jacobian contain sub matrices of log magnitude and phase,

$$\frac{\partial \ln I_i}{\partial D_j}, \frac{\partial \ln I_i}{\partial \mu_j}, \frac{\partial \theta_i}{\partial D_j}, \frac{\partial \theta_i}{\partial \mu_j}$$

which indicates elements of sub matrices for i^{th} measurement and j^{th} reconstruction node. The Jacobian is formed using adjoint method. Inverse solving is done using NIRFAST.

5. Results and Discussion

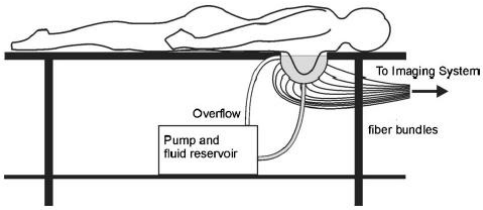

Figure 5. A schematic of the breast imaging table and liquid-circulating mechanism [8]

A model of 3D breast imager is simulated using COMSOL. The breast is placed in a hemispherical cup surrounded by sources and detectors, and the remaining space is filled with a fluid with tissue-like optical properties [8] as modeled as in figure 5.

The 3D cup imager is shown in figure 6a and 6b. Optic fiber bundles are connected to the cup for excitation and for detecting photon density. Sources are placed one scattering length inside the boundary and detectors at boundary. Source fibers are excited with LEDs of wavelength 754nm which is modeled as point source as shown in figure 6c. The excitation and emission is modeled with 3 inhomogeneities-one absorber, one scatterer and a blob of fluorescent dye. The dye properties are used to model emission. Topographical slices are used to visualize the 3D solution of excitation and emission models as shown in figure 6c and 6d.

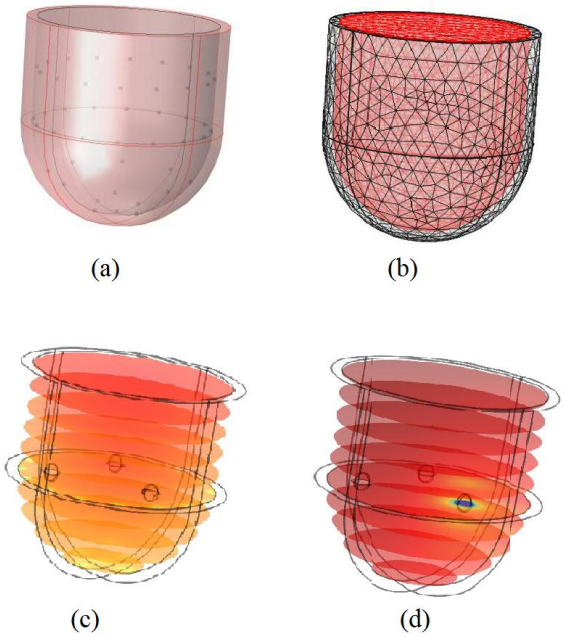

Figure 6. (a) Cup shaped imager with source location (b) FEM mesh for the cup (c) Imager excited with 754nm LEDs modeled as point source (d) Reemission from the fluorescent dye at 787nm

Computing time for one forward solving using Newton Raphson's method with fully coupling and segregation coupling as given in the table 1.

Table 1: Computing time

Method of coupling	Time (s)
Segregation coupling	19
Fully coupling	9

The result shown in the table above clearly indicates that fully coupling the two equations will reduce computing time. Reconstruction is done for one tomographic slice. At 16 detector locations the photon fluence is extracted for each source, excited one at a time and an array of measured value is formed using adjoint method. Another 2D slice of homogenous absorption and scattering is used as initial mesh for reconstruction. This model is also excited with sources as shown and the values gathered from the detectors are used to form the calculated data set. A mismatch vector was formed taking difference of measured data and calculated data. Error is calculated and is compared to the threshold value. A Jacobian is formed and parameter updates were calculated. This process is continued until error is minimized and becomes less than the threshold or as it tends to the maximal iteration. In this way we invert the diffusion equation and optical properties, μ_a and μ'_s are reconstructed. The excitation and emission equations are independently inverted as shown in figure 7a and figure 7b. Under the assumptions taken in section 5 the only change reflected were the utility of the respective excitation and emission wavelengths for the fluorescent dye. On obtaining this the reconstructed optical properties in figure 7a and figure 7b are subtracted to yield the fluorescent dye properties and further added on to the homogenous background to obtain figure 7c.

Optical parameters for excitation and emission light are given in table 2. As depicted in the figure 7 a, b & c, the optical properties are appropriately reconstructed.

Table 2: Optical Properties

Domain	μ_a (mm-1)	μ'_s (mm-1)
Background	0.01	1
Absorber	0.02	1
Scatterer	0.01	2
Dye	0.115	2

Florescence quantum yield η of the dye is 0.114; Molar extinction coefficient ε_x of dye 6.25e5 M−1 cm−1 and lifetime τ is taken as 1

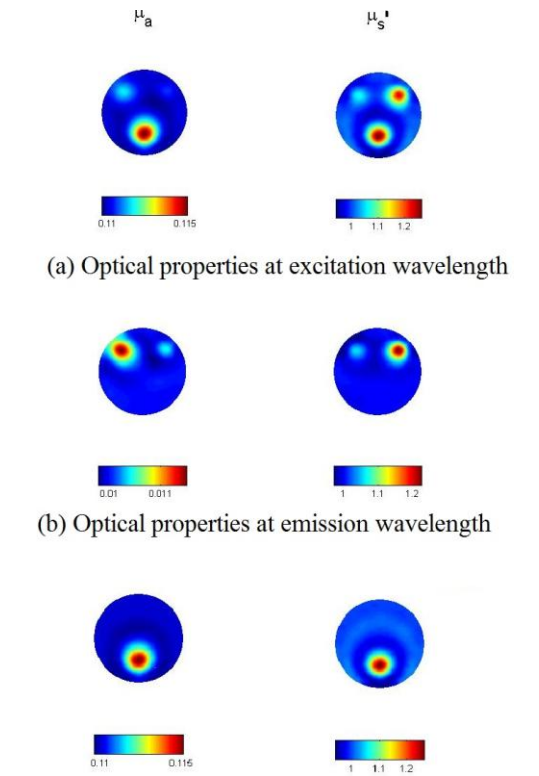

(a) Optical properties at excitation wavelength

(b) Optical properties at emission wavelength

(c) Reconstructed optical properties of fluorecent dye

Figure 7. Reconstructed optical properties

At the reconstruction the error function E between the simulated data and predicted data was computed using the formulation as given below.

$$E = \frac{1}{N} \| F(x) - y \|^2$$

Where F is forward operation, x is the reconstructed optical properties and N is the number of measurements. Error function of amplitude and phase is tabulated in Table 3.

Table 3: Error Function

Parameter	Error Function (E)
Amplitude	9.3705e-07
Phase	2.4401e-03

Table 4, shows the mean square error of optical properties μ_a and μ'_s. It is very clear from the data that we have achieved a very close reconstruction with a minute deviation from the actual properties.

Table 4: Mean square error

Parameter	MSE
μ_a	0.0024
μ'_s	0.0010

7. Conclusions

In this work we have presented the reconstruction of location and optical properties of our target specific fluorescent dye. The intensity of dye indicates more estrogen receptors in that volume which in turn gives cancerous tissue location. 2D reconstruction of tomographic slices helps in diagnosing cancer in 3D volume by moving source detector location to the area of interest. The work shows that the novel dye can be carried forth for in-vivo studies and experimental setup can be built in a laboratory for accurate diagnosis of breast cancer.

8. References

1. H. Dehghani, M.E. Eames, P.K. Yalavarthy, S.C. Davis, S. Srinivasan, C.M. Carpenter, B.W. Pogue, and K.D. Paulsen, “Near infrared optical tomography using NIRFAST: Algorithm for numerical model and image reconstruction,” Communications in Numerical Methods in Engineering, vol. 25, pp. 711-732,(2009)

2. Michael Jermyn et al. "A Seamless User-Enabling Workflow for Modeling Near-Infrared Light Transport in Tissue," OSA Biomed(2012).

3. Iven J, Gargi V, Kodand D,Uday D,"Non invasive imaging of breast cancer: Synthesis and study of novel near-infrared fluorescent estrogen conjugate", Proc.SPIE, 5693, p.521-527, (2005).

4. Shubhadeep B, Iven J, Early detection of Breast Cancer:A molecular optical imaging approach using novel estrogen conjugate fluorescent dye, Proc.SPIE,7896, 1F1-1F15,(2012)

5. Daniel J, Eva M, Sevick–Muraca, Developments towards diagnostic breast cancer imaging using Near-Infrared optical measurements and fluorescent contrast agents, Neoplasia-Nature, Vol 2, p388-417,(2000)

6. Ralf B, Jorg P, Wolfhard S, Independent modeling of fluorescence excitation and emission with the finite element method, OSA, BioMed,(2004)

7. Xiaolei Song, Ji Yi, Jing Bai, A Parallel Reconstruction scheme in Fluorescence Tomography Based on Contrast of Independent Inversed Absorption Properties, International Journal of Biomedical Imaging, 70839, p1-7, (2006)

8. Tara D, S R. Arridge, Time-resolved optical mammography using a liquid coupled interface, Journal of Biomedical Optics , Vol 10,p054011-1-10(2005)

9. A P Gibson, S R Arridge ,Recent advances in diffuse optical imaging, Phy. Med. Biol, 50, p R1- R43,(2005)